AD-A035 877 LETTERMAN ARMY INST OF RESEARCH SAN FRANCISCO CALIF F/G 6/18
OCULAR HAZARD OF THE GALLIUM ARSENIDE (GAAS) LASER.(U)
OCT 76 D J LUND, D O ADAMS, C CARVER

UNCLASSIFIED LAIR-30 NL

1 OF 1
ADA035877

END

DATE
FILMED
3 - 77

ADA035877

AD

INSTITUTE REPORT NO. 30

OCULAR HAZARD OF THE GALLIUM ARSENIDE LASER

NON-IONIZING RADIATION DIVISION
DEPARTMENT OF BIOMEDICAL STRESS

OCTOBER 1976

DDC
RECEIVED
FEB 23 1977
A

DISTRIBUTION STATEMENT A
Approved for public release;
Distribution Unlimited

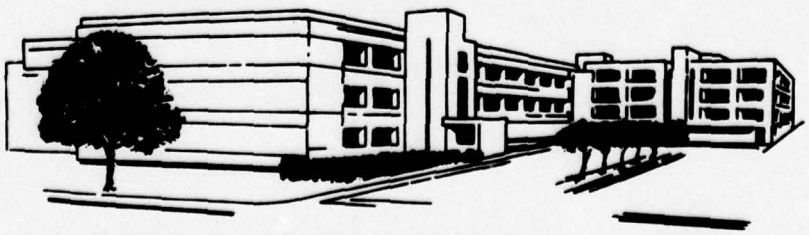

LETTERMAN ARMY INSTITUTE OF RESEARCH PRESIDIO OF SAN FRANCISCO CALIFORNIA 94129

REPRODUCTION OF THIS DOCUMENT IN WHOLE OR IN PART IS PROHIBITED EXCEPT WITH THE PERMISSION OF LETTERMAN ARMY INSTITUTE OF RESEARCH, PRESIDIO OF SAN FRANCISCO, CALIFORNIA 94129. HOWEVER, DDC IS AUTHORIZED TO REPRODUCE THE DOCUMENT FOR UNITED STATES GOVERNMENT PURPOSES.

DESTROY THIS REPORT WHEN NO LONGER NEEDED. DO NOT RETURN IT TO THE ORIGINATOR.

THE OPINIONS OR ASSERTIONS CONTAINED HEREIN ARE THE PRIVATE VIEWS OF THE AUTHORS AND ARE NOT TO BE CONSTRUED AS OFFICIAL OR AS REFLECTING THE VIEWS OF THE DEPARTMENT OF THE ARMY OR THE DEPARTMENT OF DEFENSE.

CITATION OF TRADE NAMES IN THIS REPORT DOES NOT CONSTITUTE AN OFFICIAL ENDORSEMENT OR APPROVAL OF THE USE OF SUCH ITEMS.

SECURITY CLASSIFICATION OF THIS PAGE (When Data Entered)

REPORT DOCUMENTATION PAGE

READ INSTRUCTIONS BEFORE COMPLETING FORM

1. REPORT NUMBER	2. GOVT ACCESSION NO. (9)
3. RECIPIENT'S CATALOG NUMBER (Rept.)	
4. TITLE (and Subtitle) (6) Ocular Hazard of the (GaAs) Laser. Gallium Arsenide	5. TYPE OF REPORT & PERIOD COVERED Final 1 Jan 70 - 1 Jan 75
	6. PERFORMING ORG. REPORT NUMBER
7. AUTHOR(s) (10) David J. Lund, Dolph O. Adams, ~~Ph.D.~~ Charles Carver	8. CONTRACT OR GRANT NUMBER(s)
9. PERFORMING ORGANIZATION NAME AND ADDRESS Non-Ionizing Radiation Division Department of Biomedical Stress LAIR, PSF, CA 94129 (12) 24 p.	10. PROGRAM ELEMENT, PROJECT, TASK AREA & WORK UNIT NUMBERS (16) 62758A, 3A762758A824 03 078
11. CONTROLLING OFFICE NAME AND ADDRESS Letterman Army Institute of Research Presidio of San Francisco, CA 94129	12. REPORT DATE (11) October 1976
	13. NUMBER OF PAGES 19
14. MONITORING AGENCY NAME & ADDRESS(if different from Controlling Office) U.S. Army Medical Research and Development Command Washington, D.C. 20314 (17) 03	15. SECURITY CLASS. (of this report) Unclassified
	15a. DECLASSIFICATION/DOWNGRADING SCHEDULE

16. DISTRIBUTION STATEMENT (of this Report)

Approved for public release; distribution unlimited

(14) LAIR-30

17. DISTRIBUTION STATEMENT (of the abstract entered in Block 20, if different from Report)

Unlimited

18. SUPPLEMENTARY NOTES

19. KEY WORDS (Continue on reverse side if necessary and identify by block number)

GaAs Laser, Ocular Effects, Laser Safety, Retinal Damage

20. ABSTRACT (Continue on reverse side if necessary and identify by block number)

The Gallium Arsenide (GaAs) Semiconductor laser is finding application in many devices which subject human eyes to laser irradiation. This study evaluated a single diode laboratory device to determine an ED_{50} level in rhesus monkeys. The RCA 7610 GaAs laser diode used in this experiment was cooled to cryogenic temperature (77°K) to allow rapid pulsing, thus increasing average power enough to create retinal burns.

DD FORM 1 JAN 73 1473 EDITION OF 1 NOV 65 IS OBSOLETE

404 912

SECURITY CLASSIFICATION OF THIS PAGE (When Data Entered)

The following are beam parameters measured at the eye:

Pulse Width - 500 nsec

PRR - 120 KHz

Average Power - 100 mw max

The predicted retinal spot configuration is that of an elongated rectangle 170 μ by 20 μ. Retinal burns in all cases, however, were circular in nature; and no explanation for this phenomenon has been found. It is also to be noted that pathologic examination of the retinal lesions (light microscopy) demonstrated a peculiar annular of ring shape that was unexpected. (This effect has been noted in other long pulse exposures with different wavelengths).

Four exposure durations were evaluated as follows:

Exposure Duration	.125 Sec	.5 Sec	1.0 Sec	8.0 Sec
No. of Exposures	130	198	448	285
ED_{50}, mw	55.6	37.9	39.0	19.4

TABLE OF CONTENTS

		Page
INTRODUCTION		1
MATERIALS AND METHODS		1
HISTOPATHOLOGY		4
RESULTS		
Table I		7
Table II		8
Table III		8
DISCUSSION		9
LEGEND OF FIGURES		10
Figure 1	GaAs Experimental Configuration	11
Figure 2	Far Field Pattern of Collimated GaAS Laser Beam	12
Figure 3	Collimated Beam Divergence of the GaAs Laser	13
Figure 4	Spectral Emission of the GaAs Laser a Function of Elapsed On-Time	14
Figure 5	Fundus Photograph of Rhesus Monkey Eye Showing Retinal Lesions After GaAs Irradiance	12
Figure 6	Photomicrograph of an Acute (one hour post exposure) Chorioretinal Lesion	15
Figure 7	Flat Preparation of Pigment Epithelium	15
Figure 8	The Acute Response	15
Figure 9	Retinal Damage Probability for GaAs Laser .125 Sec Exposure and .5 Sec Exposure	16
Figure 10	Retinal Damage Probability for GaAs Laser 8 Sec Exposure and 1 Sec Exposure	17
Figure 11	50% Damage Probability Power Level vs Exposure Duration	18
DISTRIBUTION LIST		19

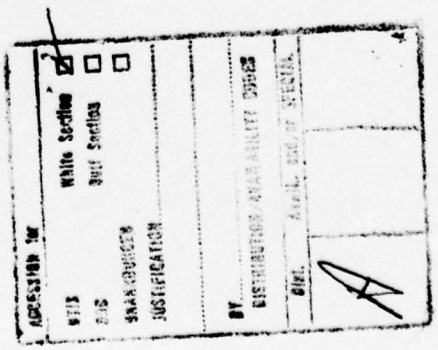

INTRODUCTION

The Gallium Arsenide (GaAs) semiconductor laser is finding application in devices which subject human eyes to laser radiation. Insufficient data existed to allow adequate determination of the ocular hazard associated with such application. The geometrical and optical characteristics of the laser produce highly divergent output radiation which must be collimated for most uses. It was the purpose of this study to produce a GaAs laser beam capable of causing retinal burns, to evaluate the beam characteristics, and to determine ocular damage threshold levels.

MATERIALS AND METHODS

An RCA 7610 GaAs laser diode served as the radiation source in all the experiments. The laser was operated in the high repetition rate mode with the operating parameters optimized for maximum average power. With the laser maintained at ambient temperature, junction heating caused by the high driving current restricted the duty cycle to 0.1% and the average power to 5 milliwatts. Cooling of the diode to cryogenic temperature enabled it to lase with lower driving current. A much higher duty cycle was possible before junction heating became significant. A power supply was designed and constructed to drive the diode to maximum output at both operating temperatures. Experiments were performed in both ranges. Typical of solid state devices, the laser required no warm-up time, delivering full output power instantly when driving current was applied. This fact was used to the advantage of laser lifetime by gating the laser on only for the exposure duration.

The exposure system is depicted in schematic form by Figure 1. The manufacturer packaged the laser diode in a threaded coaxial mount. A solid copper block comprising the cold finger of a LN cryostat was provided with a threaded hole to accept the coaxial mount, providing rigid mechanical support and good thermal contact.

The laser was oriented with the p-n junction of the diode in the horizontal plane. A simple 21.8 mm focal length lens collimated the laser emission and directed the resulting beam to a beam splitter which diverted 90% of the radiation into the experimental eye. An RCA C31000E photomultiplier detected the remainder of the beam through a diffuse transmitter. A HeNe laser beam, introduced collinearly with the GaAs laser beam, facilitated aiming and alignment.

A goniometer mount provided accurate rotation of the animal about the pupil of the eye to be exposed, allowing precise position of the exposures. The exposure sites were observed and photographed through the beam splitter via a Zeiss fundus camera. An electronic camera shutter controlled the exposure duration and provided the gate signal for the laser power supply.

Calibration of the exposure system was performed by placing the calibration standard, a TRG 100 ballistic thermopile, in the eye exposure position. Upon exposure, this detector measured the energy which would enter the eye (TIE). Simultaneously, the photomultiplier signal due to the reference beam was oscillographed, the recorded signal consisting of a superposition of all the pulses emitted by the laser during the exposure. A counter indicated the number of pulses. Within a series, the pulse width, shape, frequency, and number of pulses per exposure were held constant. Thus, the TIE was directly proportional to the peak pulse height indicated by the photomultiplier in the reference beam. Comparison to the TRG 100 output yielded the constant of proportionality. A calibration was performed each day that an animal was exposed.

The beam characteristics were investigated as a necessary part of describing the exposure system. The optics of the delivery system were chosen to deliver the maximum irradiance at the retina. The focal length of the collimating lens provided a compromise between the theoretical optimum and the physical limitations imposed by the cryogenic cooler. The uncollimated laser output lay almost entirely within a 28° square cone, producing a beam 11 mm x 11 mm at the lens. The beam produced at best collimation was 5 mm square at the eye position. Best collimation was achieved in practice by obtaining the sharpest image of the p-n junction at a distance of 7 meters, this being the nearest convenient point to infinity within the laboratory.

Given the collimator focal length of 21.8 mm and laser source dimensions of 230 μ x 2 μ, the expected beam divergence is 10.5 mr x .2 mr. A far field camera verified these expectations. The camera was positioned with the entrance aperture (coincident with the lens) at the position in the system normally occupied by the experimental eye.

The far field pattern was photographed (Figure 2) and the profile in both directions determined via densitometry. The profiles (Figure 3) are consistent with the calculated beam divergence. At threshold the entire exit aperture emits uniformly, and the far field pattern conforms to a beam divergence of 11 mr x .2 mr. At operating levels above threshold, the laser ceases to emit uniformly along the length of the junction as exhibited by the nonuniform far field pattern. During the course of the experiments the camera was apertured down to considerably smaller than the pupil of the experimental animal eyes with no degradation of image other than reduced intensity.

The spatial distribution at the focal plane of the far field camera is that which should appear at the retina of an unaccommodated emetropic eye, with a reduction in size proportional to the focal lengths. Thus, the expected retinal energy distribution is completely described.

Ancillary to the preceding was an investigation of the wavelength emitted by the laser. The output wavelength of the semiconductor laser is temperature dependent, shifting approximately 2.5 Å per °K. When the laser is first turned on there is a rapid shift toward longer wavelengths as the temperature rises to accommodate the heat created by the driving current. The wavelength stabilizes when the diode reaches thermal equilibrium. All the exposures in these experiments included the shifting portion of laser output. Therefore, the shift was experimentally evaluated.

The laser was operated at the low temperature exposure parameters (Table II). The output was directed into grating monochromater and the transmitted radiation detected with a photomultiplier. The monochromater transmission and photomultiplier sensitivity were assumed to be flat throughout the wavelength interval of interest. The monochromater was set at a wavelength within the expected output range, the laser turned on for one second, and the photomultiplier output oscillographed. After the laser recovered, the monochromater wavelength was incremented and the process repeated. The entire output band was covered in this manner. The resulting series of oscillographs represented power versus time at constant wavelength, which was then converted to power versus wavelength at constant time (Figure 4). Zero time wavelength was 8525 Å according to the manufacturer. It was not measured here. The initial shift was very rapid, stabilizing in .4 seconds at approximately 8640 Å. The bandwidth at half maximum was 26 Å.

The animals used in these experiments were rhesus monkeys (Macaca Mulatta) weighing between 2 and 5 kg. Preanesthetic medication consisted of a sedative dose of phencyclidine hydrochloride (0.25 mg/kg) intramuscular and atropine sulfate (0.2 mg) subcutaneously. Anesthesia was induced with sodium pentobarbital (approximately 5 mg/kg) via the saphenous vein. A pediatric intravenous injection set was placed into the saphenous vein to administer fluids and to facilitate additional anesthetic. The pupils were dilated with phenylephrine hydrochloride (10%) combined with cyclyopentolate hydrochoride (1%). Sutures of 3-0 silk were placed in the upper eyelid to facilitate manipulation. While the eyes were open during the experiment, physiologic saline was used to maintain good corneal transparency.

The animals were positioned in the exposure system and the fundus examined via the Zeiss fundus camera. Any abnormalities were noted. Twenty-five to thirty-six exposures were placed in a square array about the macula, utilizing suprathreshold marker burns to accurately locate the rows and columns for subsequent examination.

An absorbing filter (OD 18 at .9 μ) placed over the eyepiece of the fundus camera allowed direct observation of the exposure site during the longer exposures. Eye movement during the exposures was thus detected, and any exposure so compromised excluded from further consideration.

Detailed ophthalmoscopic examination of the exposure sites was conducted at one hour post exposure. The criteria for damage was the presence of a lesion visible via this examination. The easily visible lesions, circular and well-circumscribed, had a doughnut shape - a central punched-out area surrounded by a peripheral ring. Retinal arterioles, venules, and capillaries crossed the lesions without apparent interruption. Retinal pigment epithelium as well as choroid in the lesions appeared to have undergone alteration (Figure 5).

HISTOPATHOLOGY

Several of the exposure sites were examined by retinal flat preparation and histopathologic sections. Animals were sacrificed at periods ranging from one hour to 28 days post exposure for this study.

Histology at one hour. Damage is centered about pigment epithelium and outer segments. Pigment epithelium is generally necrotic or completely destroyed in the center of the exposed area, but occasionally it is only vacuolated or swollen. Outer segments of rods and cones are completely destroyed to form large vacuoles in the subretinal space. Discharged pigment from pigment epithelium floats free in the vacuoles. Inner segments of rods and cones are generally swollen and eosinophilic; but over areas of extensive damage to pigment epithelium, they are necrotic and even completely destroyed. Damage extends into the outer nuclear layer, which is edematous and where nuclei are swollen, shrunken, or even lost. Other retinal layers are unremarkable. Beneath damaged pigment epithelium, Bruch's membrane is swollen, eosinophilic, and pushed into the choroid. The choriocapillaris is generally obliterated and the remaining choroid is slightly inflamed.

The lesions are particularly striking in that many display the most extensive damage at the edges rather than centrally (Figure 6). In such cases, the centers of the lesions are relatively spared. At the periphery of such lesions, necrosis of pigment epithelium and vacuolization and destruction of rods and cones are prominent. Examination of these eccentric lesions on flat preparations demonstrates a central circle of unremarkable or slightly swollen pigment epithelium surrounded by a ring of completely destroyed pigment epithelium (Figure 7). Reconstruction of the lesions by serial sections confirms the doughnut configuration. In some eccentric lesions, spared outer retina is overlaid by vacuoles formed by extensive coagulative and lytic necrosis of inner segments and outer nuclear layers; this gives rise to three major foci of damage (Figure 8). The eccentric configuration was present in 41 out of 59 (70%) acute and one-day-old lesions of all power levels.

Lesions produced by the 2 x ED_{50} level of power closely resemble the above lesions but are larger (approximately 280 μ as opposed to approximately 160 μ) and characterized by more destruction. Lesions produced at the ED_{20} level of power do not conform to the above description. These lesions are difficult to detect and when found are very small (25 μ). They are characterized only by swelling, necrosis, and destruction of a few pigment epithelial cells underlying small vacuoles in the subretinal space.

One day. Lesions now have more necrosis and destruction in the center of the lesions. Pigment epithelium, inner segments, and outer segments are generally necrotic and at the periphery there is definite coagulative necrosis. Vacuoles in the subretinal space are smaller than at one hour and partially filled by necrotic debris and occasional phagocytic cells. A doughnut shape is still discernible but the central cells, which previously appeared to be spared, now display coagulative necrosis and destruction so that the entire width of damaged pigment epithelium is visibly altered.

Three to five days. Lesions are now definitely smaller. The subretinal space is almost completely filled with amorphous, coagulated debris though small irregular vacuoles are still seen. Within the subretinal space are large numbers of ameboid phagocytes, containing phagocytosed pigment and necrotic debris. The thinned overlying outer nuclear layer dips outward into the subretinal space and is edematous. Remaining nuclei in the outer nuclear layer, about half of the normal complement, are small and dark. Pigment epithelium generally has the appearance of regenerating epithelium. Bruch's membrane is still swollen and eosinophilic. The choriocapillaris is still partially obliterated, and leukocytic infiltration into the choroid remains.

Seven days and after. Lesions are considerably smaller than their original size. Pigment epithelium is still rough and irregular. Areas of the subretinal space previously occupied by vacuoles are now filled with amorphous eosinophilic material and phagocytic cells heavily laden with pigment. The overlying outer nuclear layer, which is thinned and depleted of nuclei, dips into the former vacuolar space and its nuclei remain dark and condensed. The inner nuclear layer is thickened and dips toward the depressed outer nuclear layer. The ganglion cell layer shows disruption, loss of ganglion cells, edema, nuclear dropping out, and loss of eosinophilic substance. Rods and cones surrounding the lesions appear to have no alterations. After seven days, lesions are relatively inconspicuous. Pigment epithelium is smooth and regular, but pigment in the tips of the cells is irregular and sparse. Outer retina is replaced by amorphous eosinophilic material. The outer nuclear layer remains thin. Other layers of the retina and the choroid are generally unremarkable.

RESULTS

Initial experiments were conducted with the laser maintained at ambient temperature and driven to the maximum output possible at that temperature (Table I).

Table I

(Beam Parameters Measured at Eye Position - Room Temperature Operation)

Peak Power	-	4.9 w
Pulse Width	-	250 ns
Pulse Shape	-	Square Wave
PRR	-	5000 Hz
Energy	-	1.05 μj/pulse
Average Power	-	5.25 mw
λ	-	9050 Å

Ten exposures were placed in the eyes of two rhesus monkeys. Exposure duration consisted of 2 at 1 second each and 8 at 32 seconds each. No lesions were detected by ophthalmoscopic or pathologic examination.

All subsequent experiments were performed with the laser maintained at 77°K (Table II).

Table II

(Beam Parameters Measured at Eye [77°K])

Peak Power	-	1.4 w max.
Pulse Width	-	500 ns
Pulse Shape	-	∿ Square
PRR	-	120 KHz
Average Power	-	100 mw max.
λ	-	8525 Å to 8640 Å

Threshold data was obtained at exposure durations of .125, .5, 1 and 8 seconds, with pulse width and repetition rate held constant. The data was subjected to exact probit analysis, the results of which are given in Table III and Figures 9 and 10.

Table III

Exposure Duration		.125 Sec	.5 Sec	1.0 Sec	8.0 Sec
No. of Animals		4	5	7	5
No. of Eyes		5	7	13	7
No. of Exposures		130	198	448	285
ED_{50}	(Energy)	7.0 mj	19.0	39.0	155.4
	(Power)	55.6 mw	37.9	39.0	19.4
$ED_{0.1}$	(Energy)	4.0 mj	5.1	17.5	55.9
	(Power)	32 mw	10.2	17.5	7.0
Lowest Burn	(Energy)	6.6 mj	13.4	28.6	131
	(Power)	52.8 mw	26.8	28.6	16.4

The ED_{50} level is plotted as a function of exposure duration in Figure 11.

DISCUSSION

Ocular damage threshold levels for the GaAs laser were determined. The experiment was sufficiently defined to predict a rectangular retinal irradiation geometry. The retinal burns were in all instances circular in shape when viewed ophthalmoscopically, and were frequently annular in shape in retinal flat preparation and histopathological section. Several possible explanations for this discrepancy exist. Perhaps a precisely rectangular retinal image was not delivered. Although all eyes were refracted in the visible, no correction was made for the 860 nm wavelength. It is possible that a lensing effect could be generated by thermal gradients near the retinal exposure. The lesions may represent choroidal reactions to radiation altered by the superficial retinal layers. The retinal response may be a result of the pulse repetition frequency of the input radiation. Additional exposure data with similar beam characteristics using other laser wavelengths may add insight to the results of this experiment.

NOTE

"In conducting the research described in this report, the investigator(s) adhered to the 'Guide for Laboratory Animal Facilities and Care' as promulgated by the Committee on the Guide for Laboratory Animal Facilities and Care, of the Institute of Laboratory Animal Resources, National Academy of Sciences - National Research Council."

LEGEND OF FIGURES

Figure 1 GaAs Experimental Configuration

Figure 2 Farfield pattern of collimated GaAs laser beam. Upper photo shows pattern with laser operated at threshold. Lower photo shows pattern with laser operated at 2X threshold.

Figure 3 Collimated Beam Divergence - GaAs Laser

Figure 4 Spectral emission of the GaAs laser as a function of elapsed on-time. The laser is turned on at time 0.

Figure 5 Fundus photograph of rhesus monkey eye showing retinal lesions after GaAs irradiation.

Figure 6 Photomicrograph of acute (one hour post exposure) chorioretinal lesion. Damage is centered upon pigment epithelium and rods and cones which are mostly necrotic. Note relative sparing of pigment epithelium centrally and complete destruction of pigment epithelium peripherally. (Hematoxylin and eosin, x500.)

Figure 7 Flat preparation of pigment epithelium demonstrates the doughnut configuration. Complete destruction of pigment epithelium periphery is centered about a core of unaltered epithelium. (Unstained, x125.)

Figure 8 The acute response. This section typifies those lesions characterized by three major loci of damage. Two major loci are centered on the pigment epithelium and a third locus is in the outer nuclear layer and superficial rods and cones. Between the three loci, rods and cones are swollen but not destroyed. Note extension of the damage into the outer plexiform layer. (Hematoxylin and eosin, x500.)

Figure 9 Retinal damage probability for GaAs laser 0.125 sec exposure and 0.5 sec exposure.

Figure 10 Retinal damage probability for GaAs laser 1 sec and 8 sec exposure.

Figure 11 Fifty percent probability level versus exposure duration.

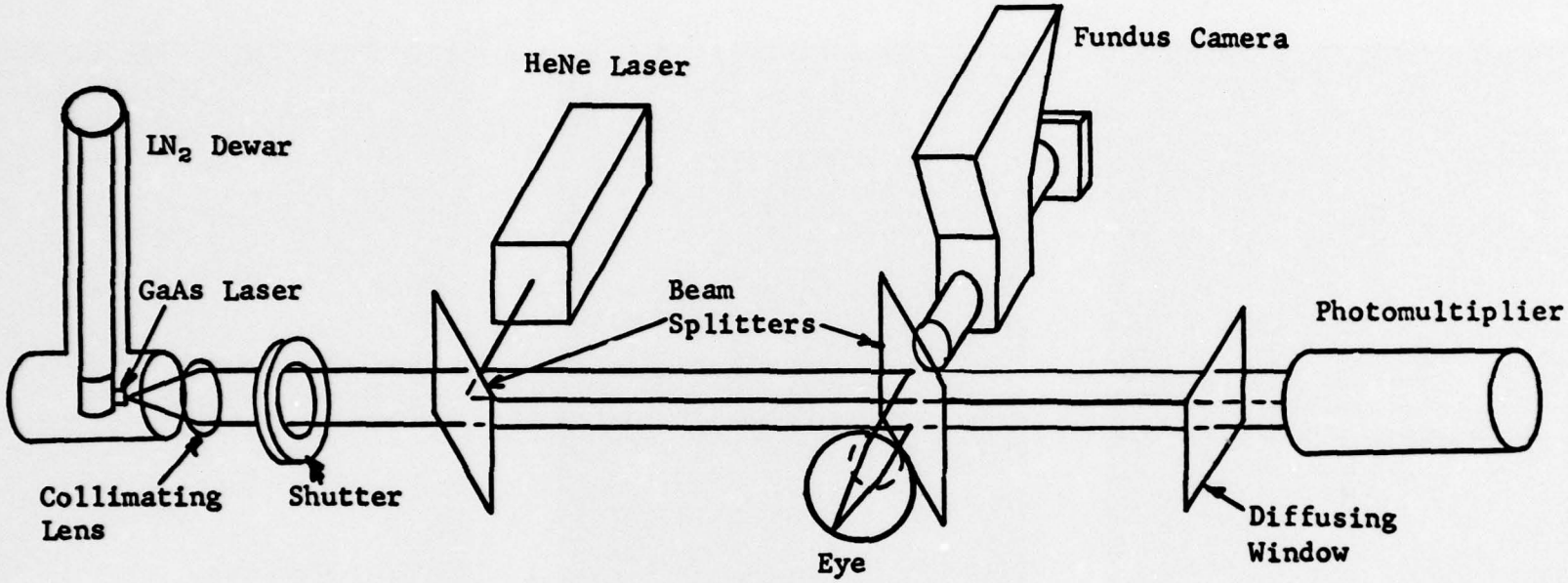

GaAs EXPERIMENTAL CONFIGURATION

Figure 1

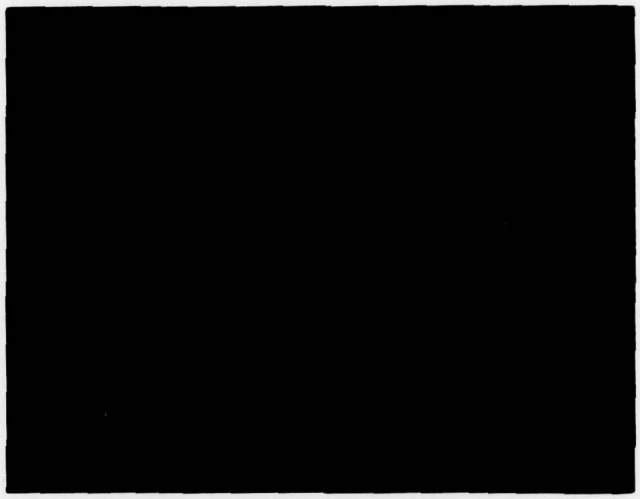

Figure 2

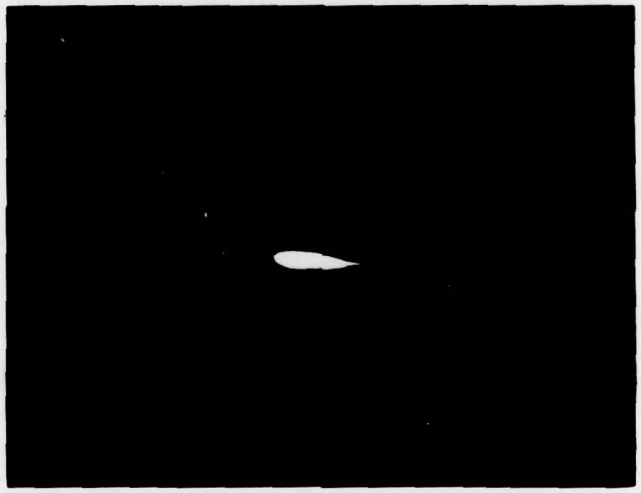

Figure 2

Figure 5

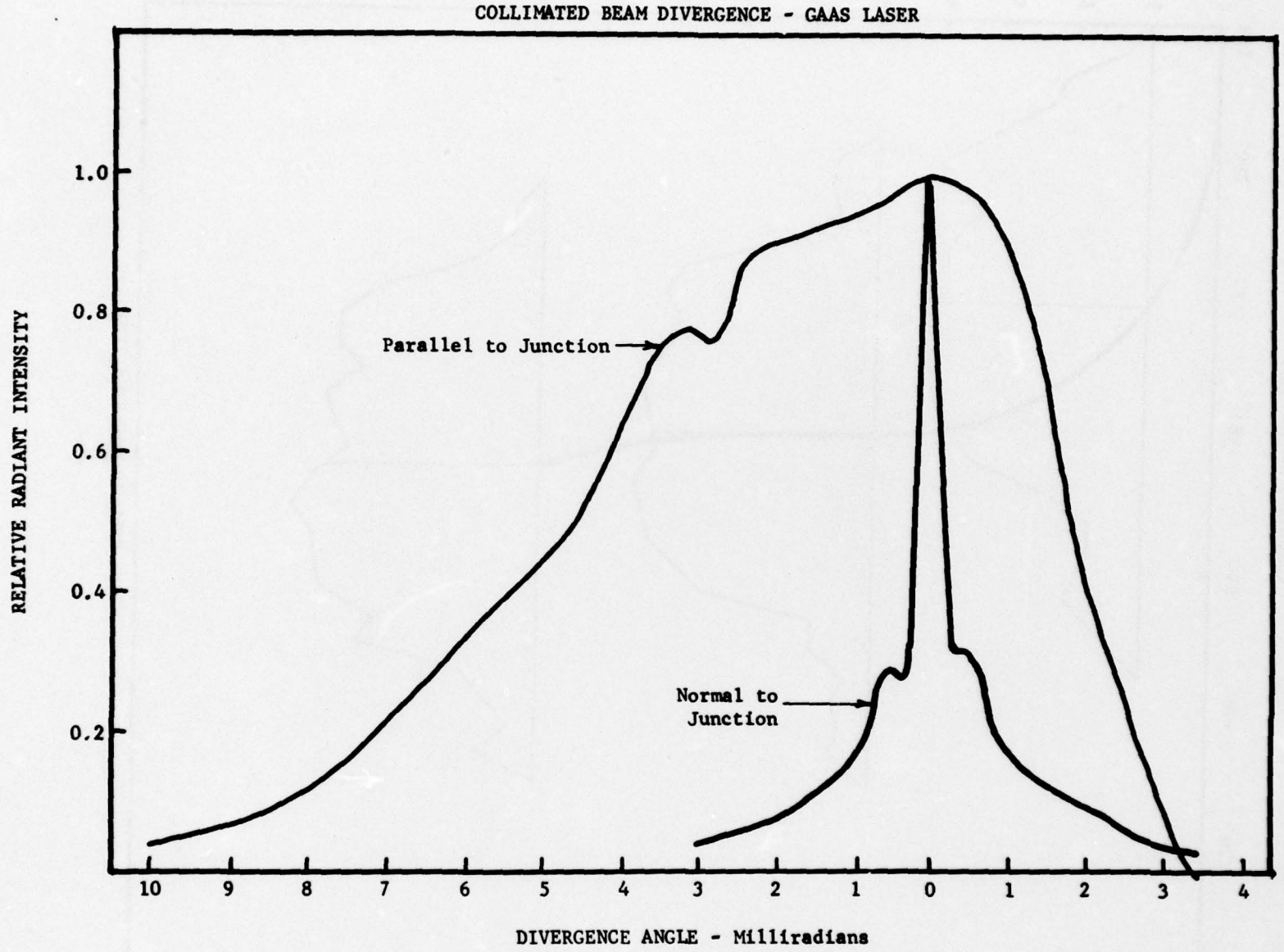
COLLIMATED BEAM DIVERGENCE - GAAS LASER
RELATIVE RADIANT INTENSITY
1.0
0.8
0.6
0.4
0.2
Parallel to Junction
Normal to Junction
10
9
8
7
6
5
4
3
2
1
0
1
2
3
4
DIVERGENCE ANGLE - Milliradians

Figure 3

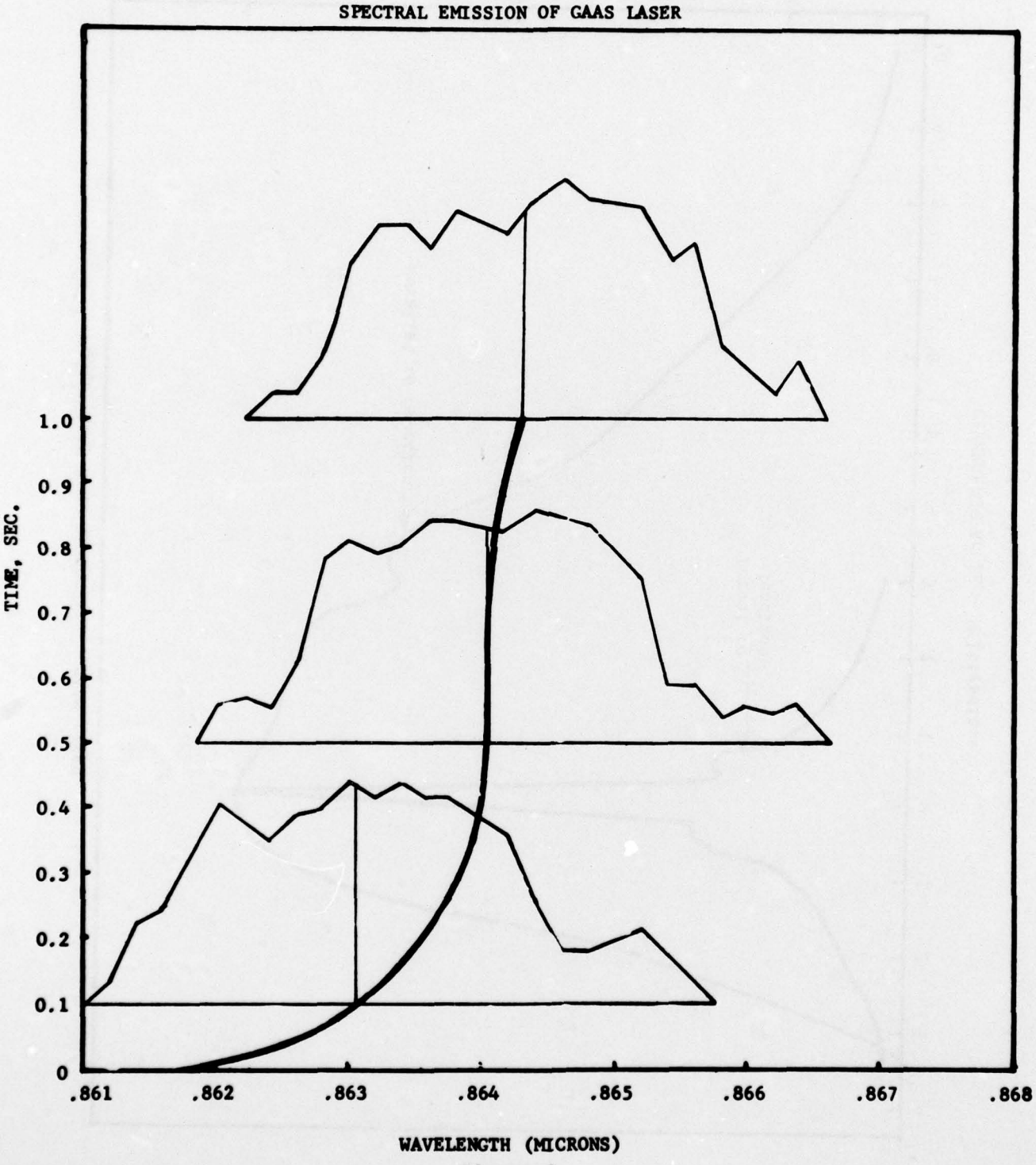
SPECTRAL EMISSION OF GAAS LASER
TIME, SEC.
1.0
0.9
0.8
0.7
0.6
0.5
0.4
0.3
0.2
0.1
0
.861
.862
.863
.864
.865
.866
.867
.868
WAVELENGTH (MICRONS)

Figure 4

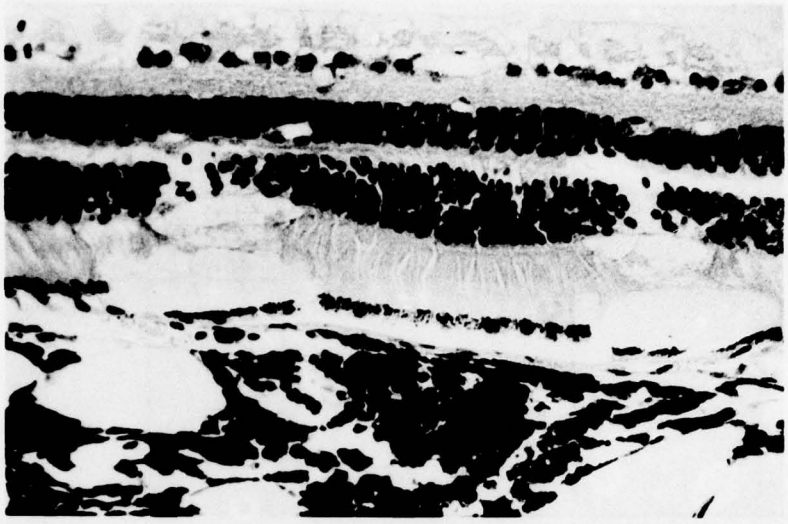

Figure 6

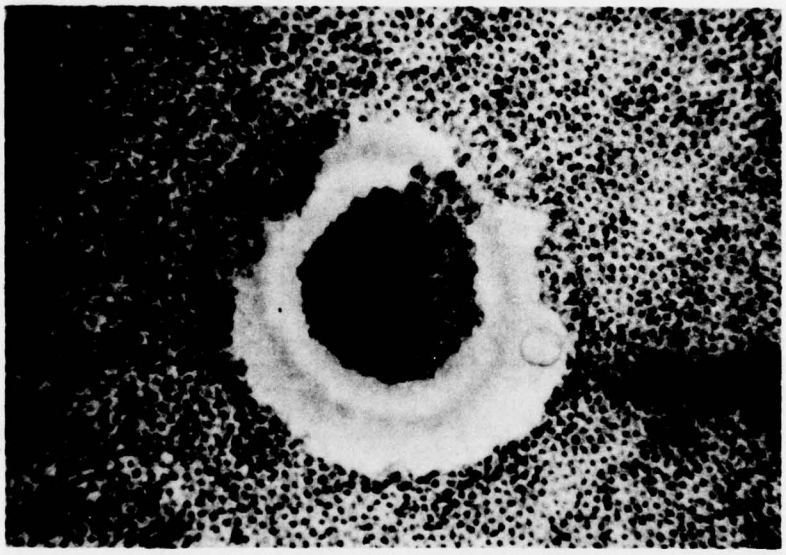

Figure 7

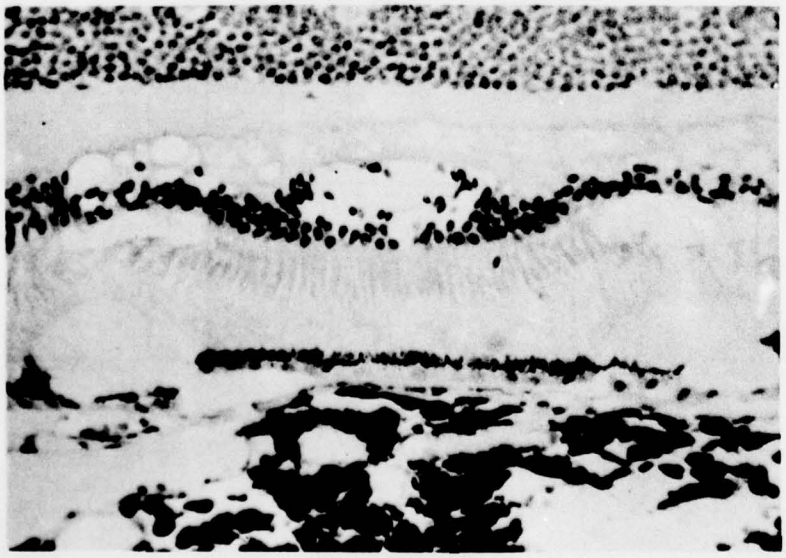

Figure 8

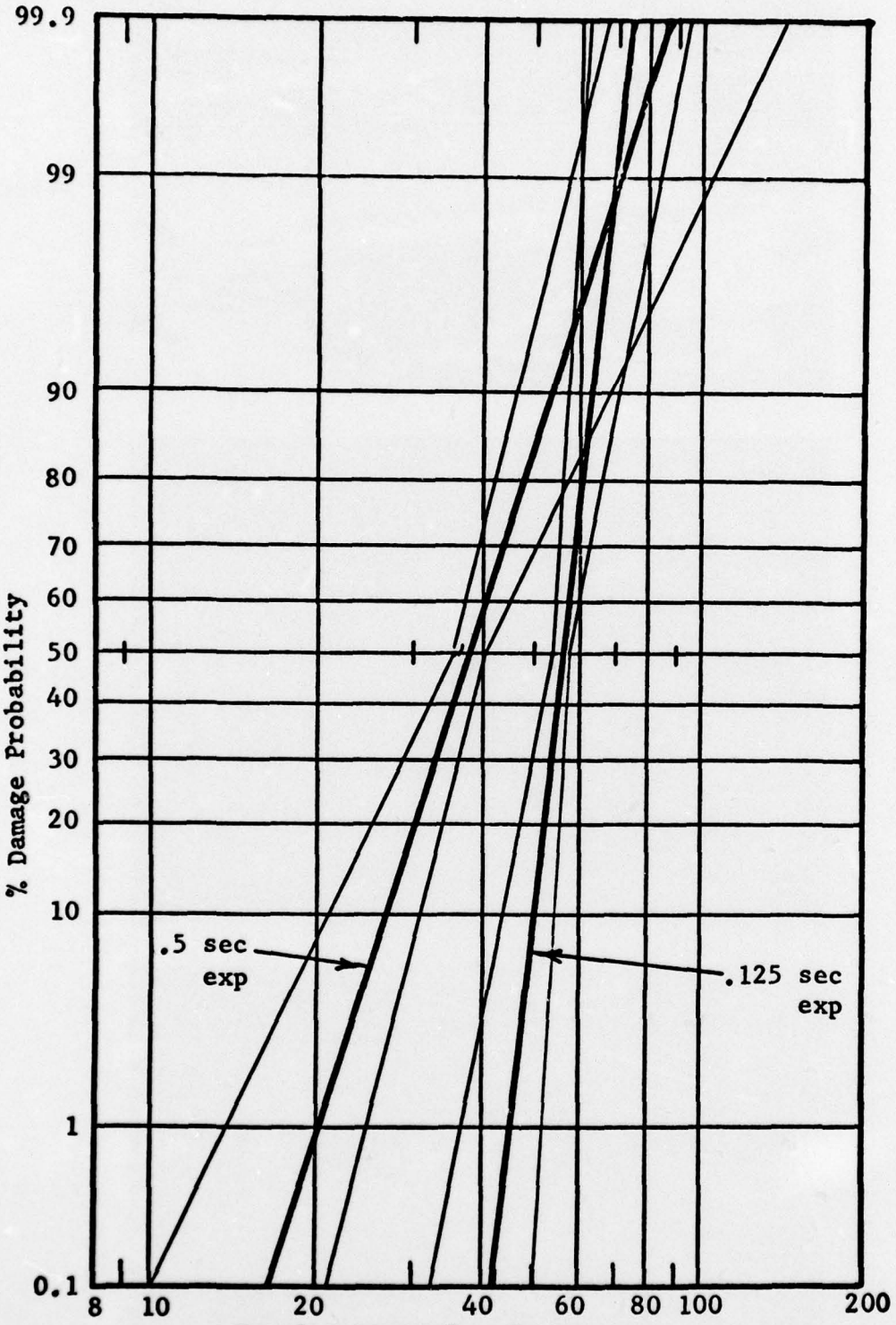

RETINAL DAMAGE PROBABILITY FOR GaAs LASER
•125 sec exposure and .5 sec exposure

Figure 9

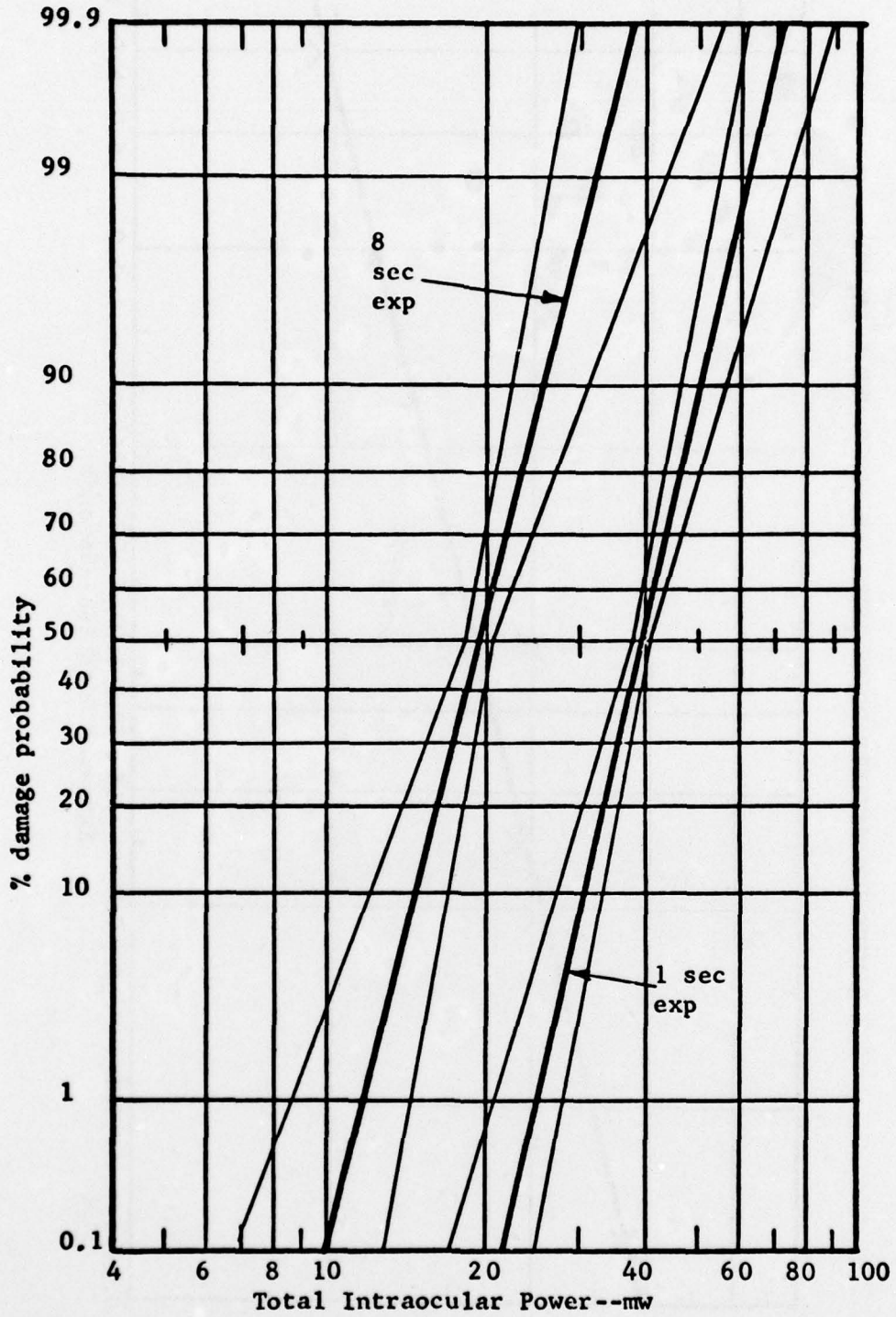

RETINAL DAMAGE PROBABILITY FOR GaAs LASER
8 sec exposure and 1 sec exposure

Figure 10

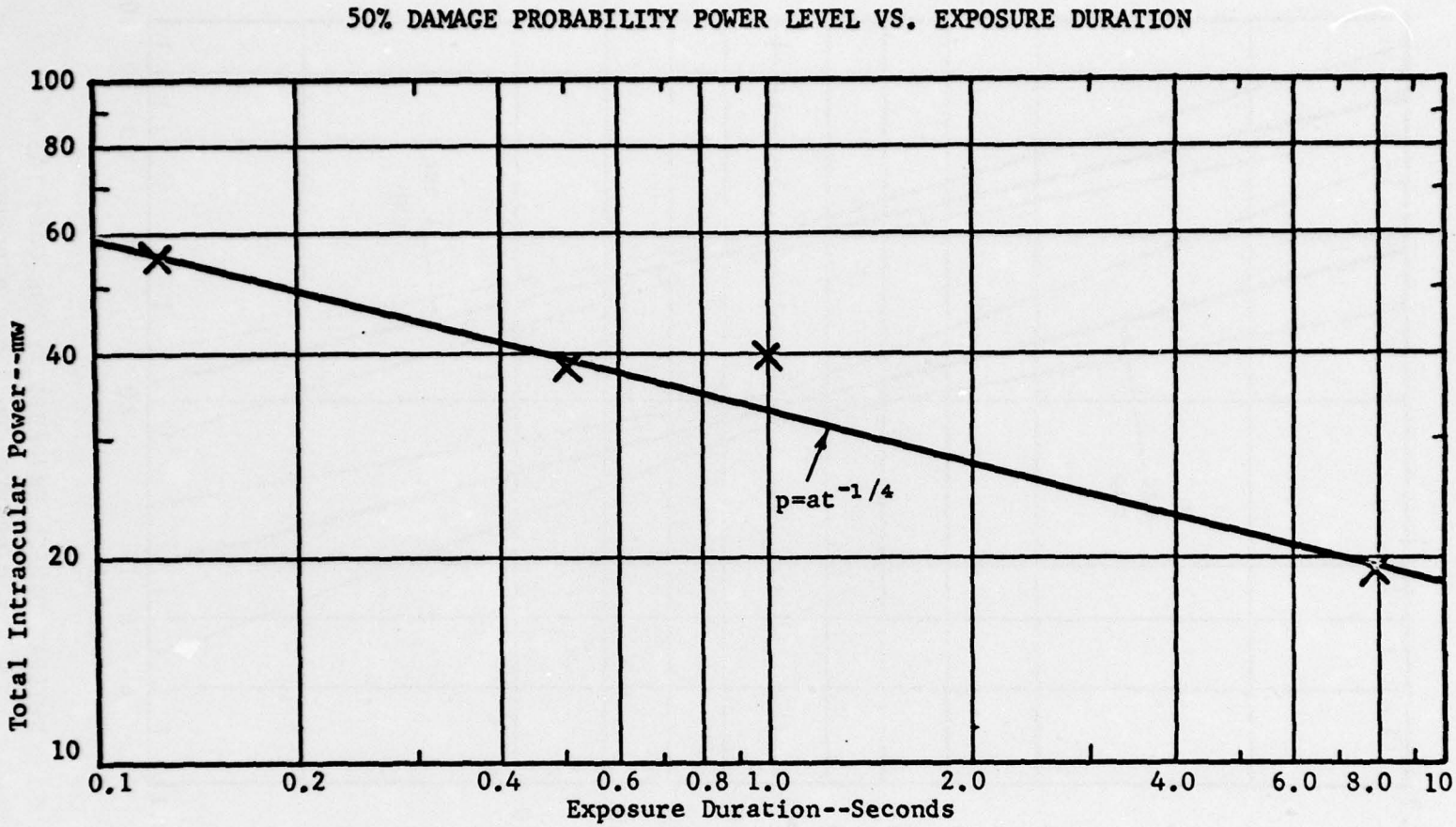
50% DAMAGE PROBABILITY POWER LEVEL VS. EXPOSURE DURATION
Total Intraocular Power--mw
100
80
60
40
20
10
0.1
0.2
0.4
0.6
0.8
1.0
2.0
4.0
6.0
8.0
10
Exposure Duration--Seconds
p=at^-1/4

Figure 11

DISTRIBUTION LIST

U.S. Army Medical Research and Development Command
Washington, DC 20314

Defense Documentation Center (12)
ATTN: DDC-TCA

Superintendent
Academy of Health Sciences, U.S. Army
ATTN: AHS-COM
Fort Sam Houston, TX 78234

Dir of Defense Research and Engineering
ATTN: Asst Dir (Environmental and Life Sciences)
Washington, DC 20301

☆GPO 789-860-1977